Maximum Entropy Tomography of 4D Transverse Phase Space Distribution with Linear and Nonlinear Projections

Liwen Liu

Institute of Modern Physics,

Chinese Academy of Sciences

Background: Significance of High-Dimensional Phase Space Reconstruction

- Simple prediction of beam dynamics from 2D projections introduces significant errors

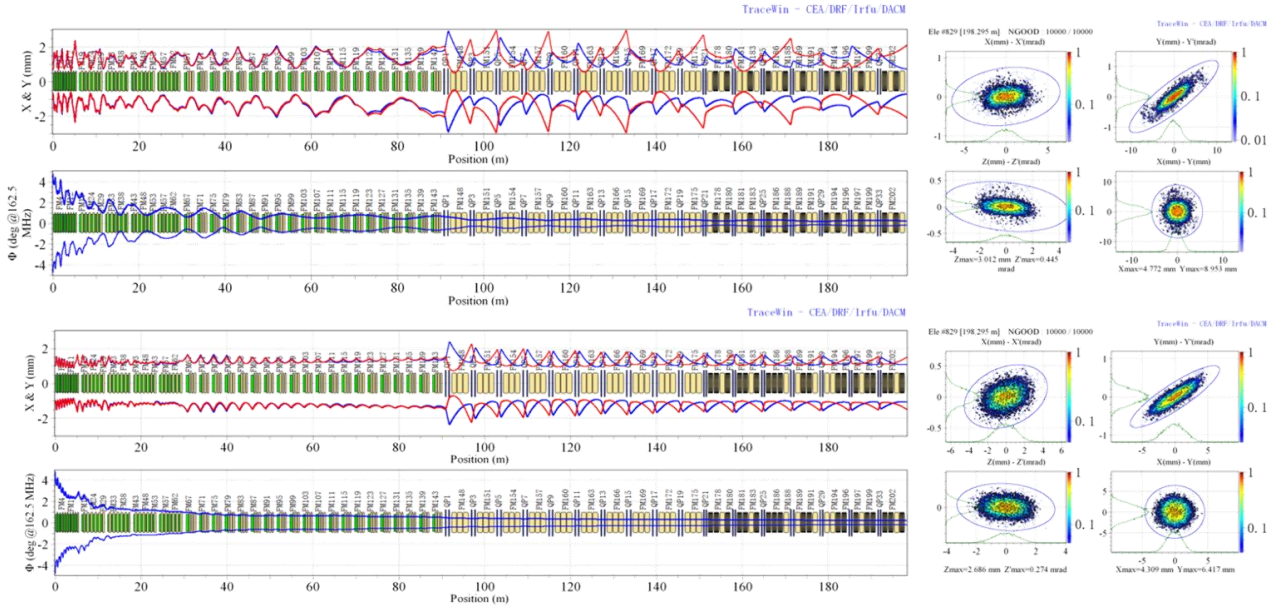

RMS evolution of independent x/y distributions VS coupled x-y distribution along the longitudinal direction

- Absence of coupling ≠ transverse plane independence

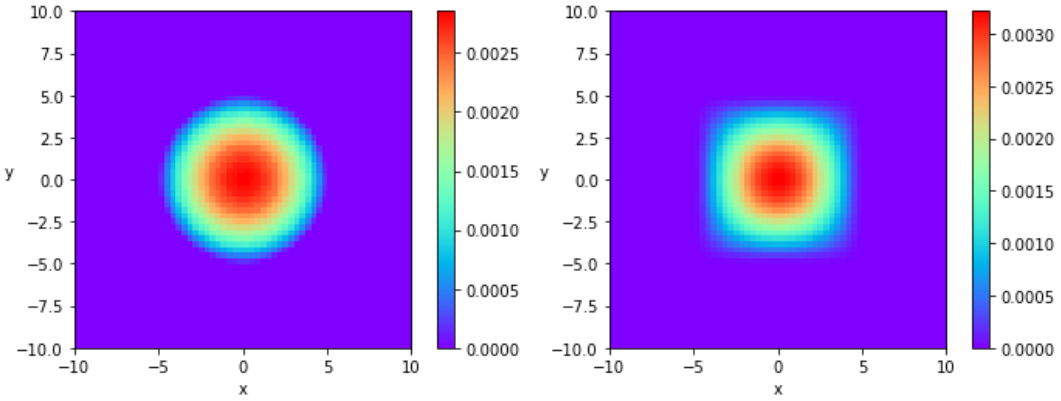

(x,y)-plane projection of the 4D phase space density $\rho(x,x',y,y')$

(x,y)-plane projection of the separable 4D distribution $\rho^*(x,x',y,y')$

$$\rho_1(x,x')=\iint \rho(x,x',y,y')\,dydy'$$

$$\rho_2(y,y')=\iint \rho(x,x',y,y')\,dxdx'$$

$$\rho(x,x',y,y') \neq \rho_1(x,x')\rho_2(y,y')$$

Complete high-dimensional beam phase space information enables precise beam loss prediction

Background: About Tomography

- Tomography:A Method for Reconstructing High-Dimensional Distributions from Low-Dimensional Projections
  - (e.g., Medical CT)
- Characteristics and Challenges of 4D Transverse Phase-Space Tomography:
  - Limited number of measurements
  - High dimensionality of the target distribution
  - Measured projections are often two dimensions lower than the reconstructed distribution
- No unique solution exists
  - A finite number of projections corresponds to multiple possible high-dimensional distributions
  - Finding the most plausible solution
- Maximum-Entropy Phase-Space Tomography:
  - Based on clear logic:
    identifying the unique solution that maximizes entropy
  - Particularly suitable for cases with sparse projection data

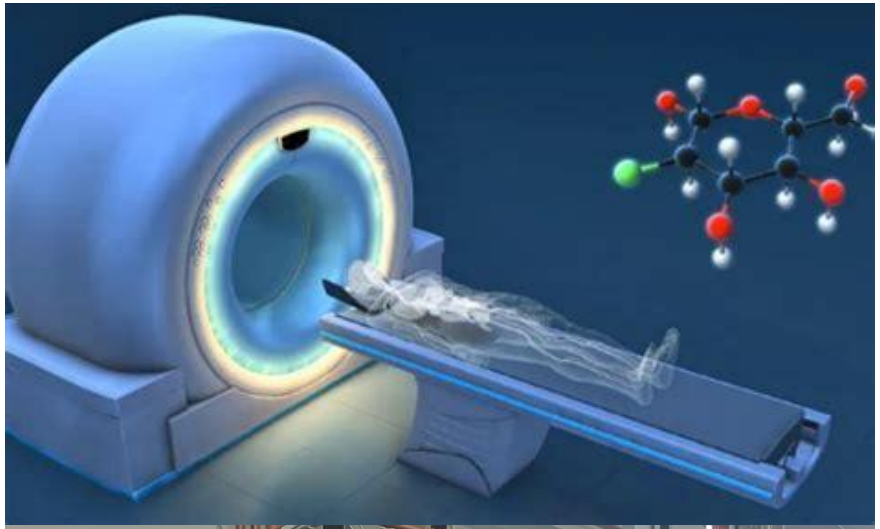

Background: About Maximum-Entropy Tomography

- Los Alamos National Laboratory proposed a tomography method based on the maximum entropy principle, achieving reconstruction from 1D to 2D

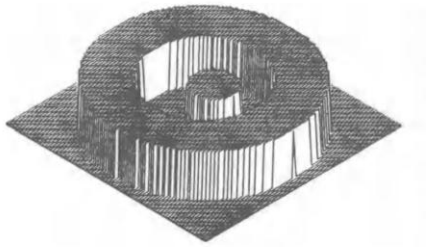

Original image

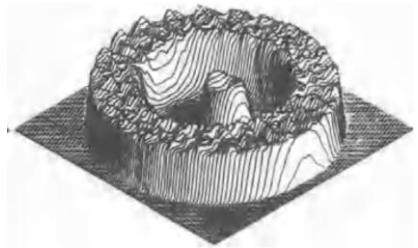

Reconstructed image

Mottershead, C.T. (1996). Maximum Entropy Tomography. In: Hanson, K.M., Silver, R.N. (eds) Maximum Entropy and Bayesian Methods. Fundamental Theories of Physics, vol 79. Springer, Dordrecht.

- **Maximum-Entropy Tomography**
  - Suited for tomography under sparse data constraints
  - Selects the distribution with maximal microscopic configurations satisfying given macroscopic measurements

SNS achieved the first reconstruction from 2D to 4D using maximum entropy methods: applicable only to direct projections

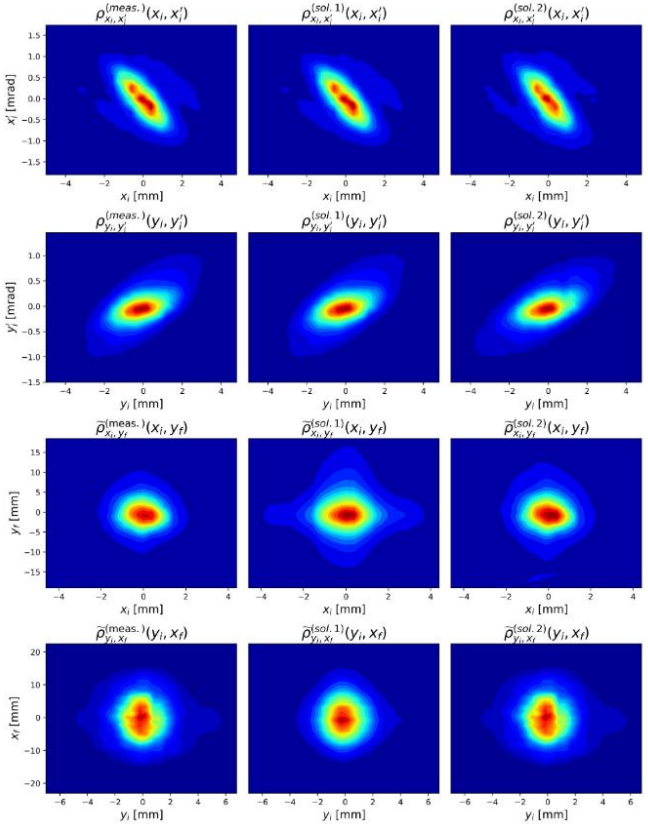

Measured 2D profiles in SNS's HEBT section (left column)
Reconstruction results using two profiles (middle column)
Reconstruction results using four profiles (right column)

Wong, J. C., Shishlo, A., Aleksandrov, A., Liu, Y., & Long, C. (2022). *4D transverse phase space tomography of an operational hydrogen ion beam via noninvasive 2D measurements using laser wires*. Physical Review Accelerators and Beams, 25, 042801.

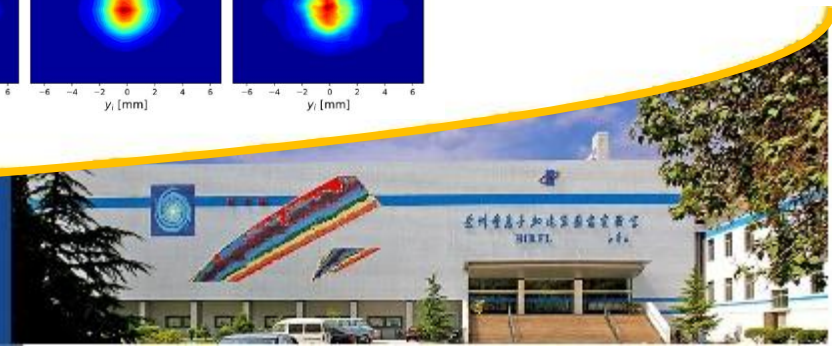

Background: Maximum Entropy Tomography(MENT) Theory from 2D to 4D

- Entropy in 4D Transverse Phase Space
  - $H[\rho] = -\iiiint \rho(x,x',y,y') \ln \rho(x,x',y,y')\, dxdx'dydy'$
  - $\rho(x,x',y,y')$: Probability density
- Constraints:
  - $G_j = g_j(u_j,u_j') - \iiiint \rho(u_j,u_j',v_j,v_j')\, dv_j dv_j' = 0$
  - $g_j(u_j,u_j')$: Measured j-th profile
  - (u_j,u_j'): Direction of the j-th profile
- Coordinate transformation:

$$\begin{bmatrix} u_j \\ u_j' \\ v_j \\ v_j' \end{bmatrix} = A_j \begin{bmatrix} x \\ x' \\ y \\ y' \end{bmatrix} = MM_j \begin{bmatrix} x \\ x' \\ y \\ y' \end{bmatrix}$$

  - $A_j = MM_j$
  - M_j: transmission matrix from the measurement points to the reconstruction points for the j-th profile
  - M: Mapping matrix from phase space to measurement coordinates
- Optimization for extremum points
  - $K[\rho] = H[\rho] + \sum_{j=1}^{n} \iint \lambda_j(u_j,u_j') G_j[\rho]\, du_j du_j'$
  - $\left.\frac{\partial K[\rho]}{\partial \rho}\right|_{\rho=\rho^*} = -\iiiint \ln \rho^* + 1 + \sum_{j=1}^{n} \lambda_j(u_j,u_j')\, dxdx'dydy' = 0$
- Solution form:
  - $\rho^* = C \cdot exp\left(-\sum_{j=1}^{n} \lambda_j(u_j,u_j') - 1\right)$
    $= C \cdot \prod_{j=1}^{n} h_j(u_j,u_j')$
  - Satisfy the constraints
  - Maximize the entropy
  - The solution takes the form of a product of component functions

Universal Algorithm for 2D-to-4D Reconstruction Based on MENT

n constraints ⟶ *n coupled nonlinear equations*

$$g_k(u_k,u'_k)=\iint \rho\, dv_k dv'_k = C_2 h_k(u_k,u'_k)\iint \prod_{j=1,j\neq k}^{n} h_j(u_j,u'_j)\, dv_k dv'_k$$

Numerical Solution of n Component Functions $h_j(u_j,u'_j)$

$$h_k^{(m+1)}(u_k,u'_k)=\frac{g_k(u_k,u'_k)}{C_2 \iint \prod_{j=1}^{k-1} h_j^{(m+1)}(u_j,u'_j)\ \prod_{j=k+1}^{n} h_j^{(m)}(u_j,u'_j)\, dv_k dv'_k}$$

Mapping all $h_j(u_j,u'_j)$ *to* (v_k,v'_k) *plane for discrete bivariate integration*

- Measured quantity: $g_k(u_k,u'_k)$
- Unknown quantity: $h_k(u_k,u'_k)$
- Solution method: Iteration

$$\rho = C\cdot\prod_{j=1}^{n} h_j(u_j,u'_j)$$

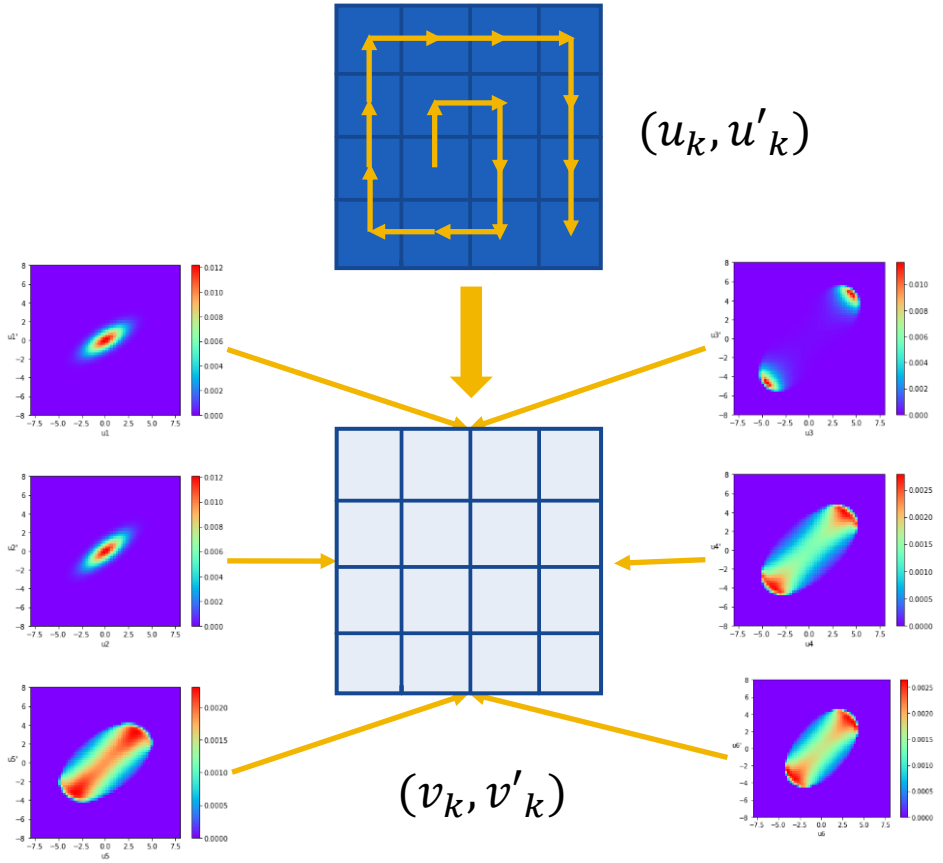

In the k-th coordinate system, we multiply the functions from the other n-1 distinct coordinate systems and then integrate

Reconstruction Algorithm Verified by Simulation

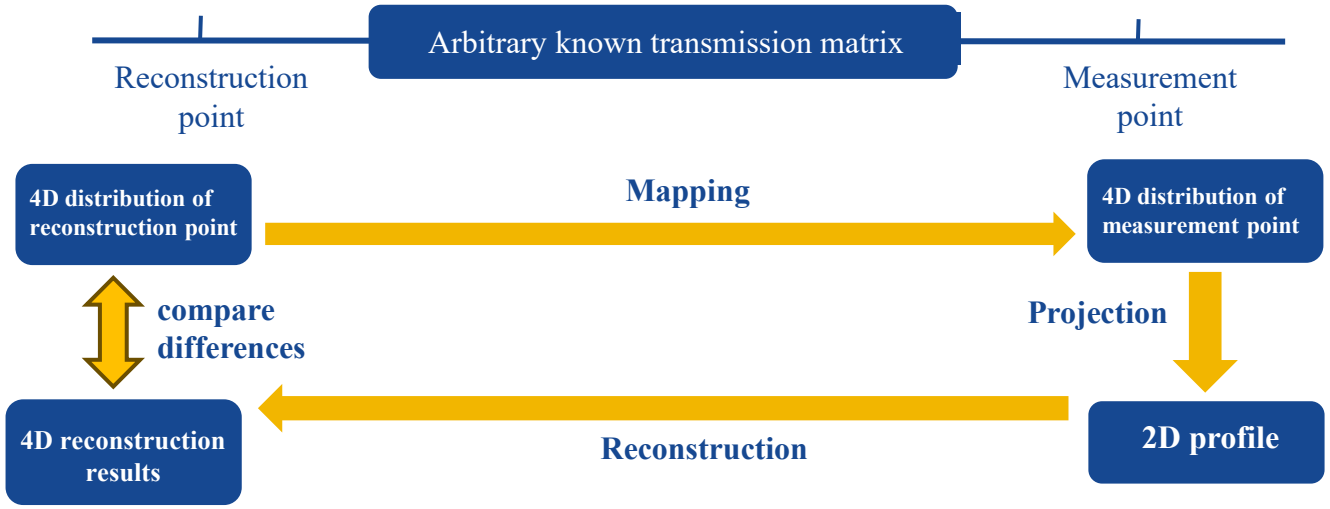

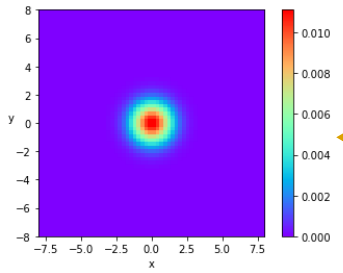

Simple reconstruction from two profiles

$$\iint \rho^*(x,x',y,y')\,dxdy$$

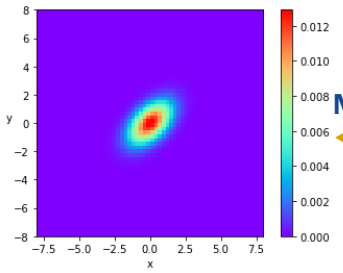

Analytical distribution

$$\iint \rho_0(x,x',y,y')\,dxdy$$

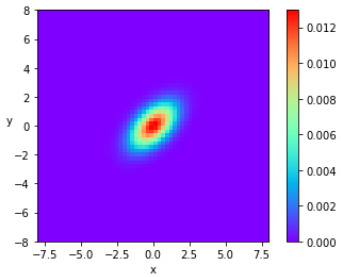

Reconstruction via maximum entropy principle

$$\iint \rho_{Re}(x,x',y,y')\,dxdy$$

M=0.2898

M=0.01622

- Reconstructed 4D Gaussian distribution $\rho_0(x,x',y,y')$ using six 2D profiles
  - ✓ Measurement point=Reconstruction point
  - ✓ Measurement point≠Reconstruction point
- The output $\rho_{Re}(x,x',y,y')$ is a four-dimensional probability density function (PDF)
- Compare with $\rho^*(x,x',y,y') = \rho_1(x,x')\rho_2(y,y')$
  - $\rho_1(x,x')=\iint \rho(x,x',y,y')\,dydy'$
  - $\rho_2(y,y')=\iint \rho(x,x',y,y')\,dxdx'$
  - Maximum entropy reconstruction contains more complete information
- Compare the differences between $\rho_{Re}(x,x',y,y')$ and $\rho_0(x,x',y,y')$
  - $D_{TV} = \frac{1}{2}\int\int\int\int|\rho_0 - \rho_{Re}|\,dxdx'dydy'$
  - $0 \le D_{TV} \le 1$
  - $D_{TV} \approx 0.0176$

Reconstruction incorporating nonlinear mapping : Iterative formula change

- First extension of maximum-entropy tomography to nonlinear reconstruction
  - More general maximum-entropy reconstruction
  - Applicable when nonlinear elements exist between reconstruction and measurement points
- Iterative formula better suited for nonlinear cases

$$h_k^{(m+1)}(u_k,u_k') = \frac{g_k(u_k,u_k')h_k^{(m)}(u_k,u_k')}{h_k^{(m)}(u_k,u_k')\iint C\prod_{j=1}^{k-1}h_j^{(m+1)}(u_j,u_j')\prod_{j=k+1}^{n}h_j^{(m)}(u_j,u_j')\,dv_k dv_k'}$$

- Key Differences from Linear Case
  - It is no longer necessary to explicitly specify the mapping relationships between the coordinate systems of each component function
  - All $f_j(x,x',y,y')$ and their inverses must be input
  - More general: any invertible mapping but not just matrixes

$$(u_j,u_j',v_j,v_j') = f_j(x,x',y,y')$$

Reconstruction incorporating nonlinear mapping : test by simulation

- Algorithm feasibility verified
  - Reconstructed distribution ρ_0 using 12 profiles
  - Simulated sextupole magnet scanning experiment
  - Successfully reconstructed 4D distribution ρ_1 via nonlinear-transport profiles

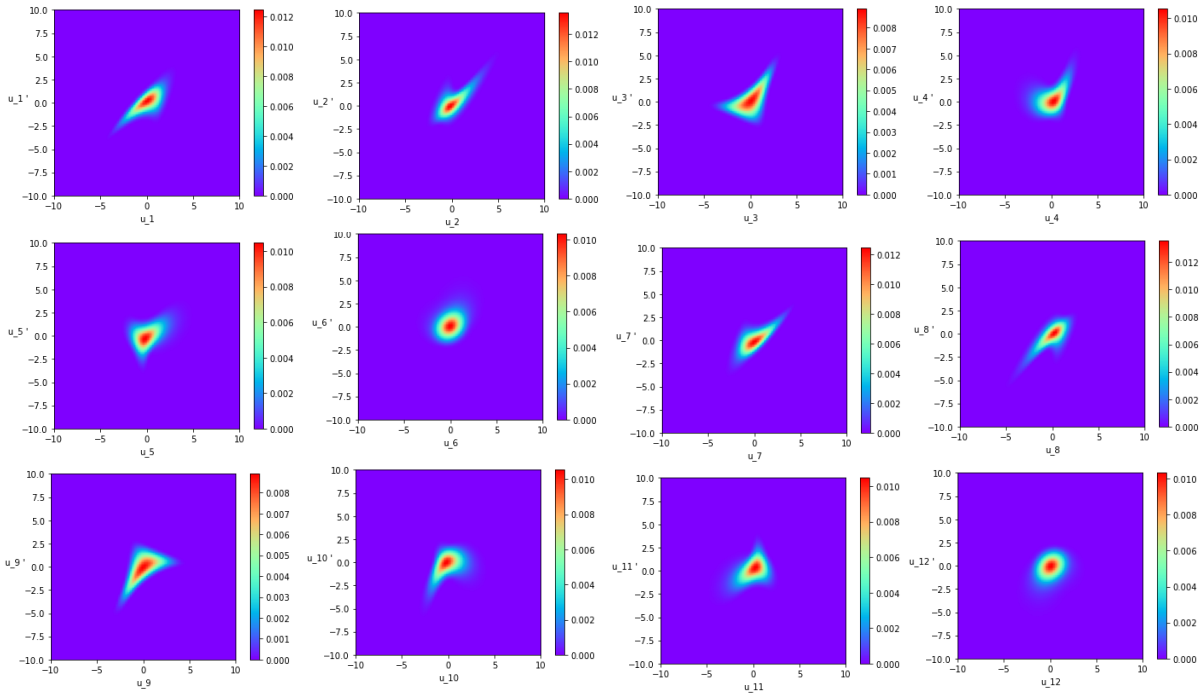

Profiles used in testing

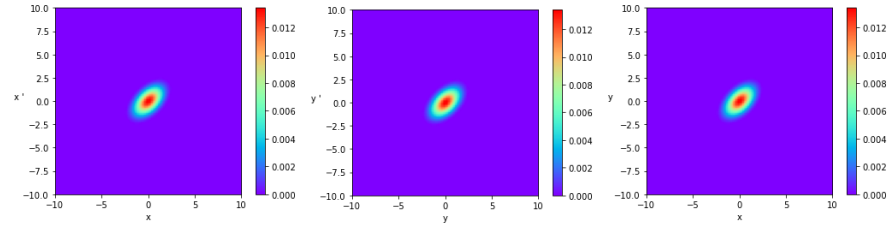

Analytical distribution ρ_0 projections

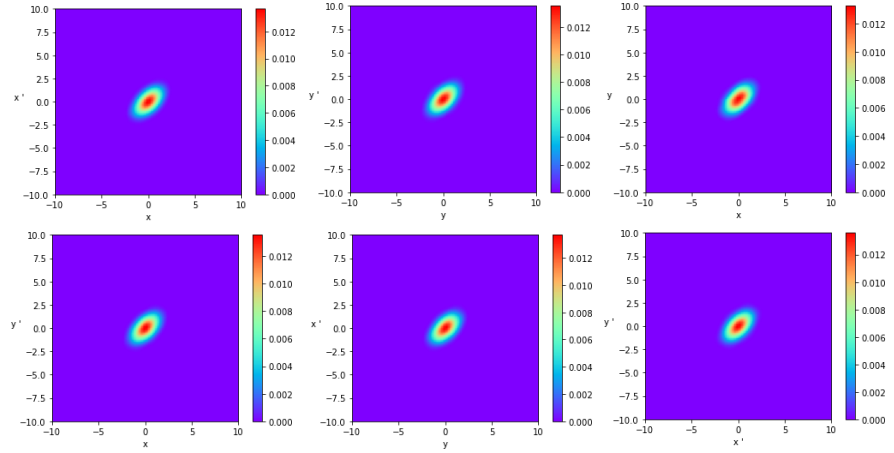

Reconstructed distribution ρ_1 projections

$$D_{TV} = \frac{1}{2}\int\int\int\int |\rho_0 - \rho_1|\, dxdx'dydy' = 0.059$$

Experiment: About CAFE-II

- Chinese Accelerator Facility for super heavy Elements (CAFE2)
  - Developed by Institute of Modern Physics (IMP), Chinese Academy of Sciences (CAS)
  - China's first continuous-wave superconducting heavy-ion accelerator
  - Upgraded from the original CAFe (China ADS Frond-end) facility

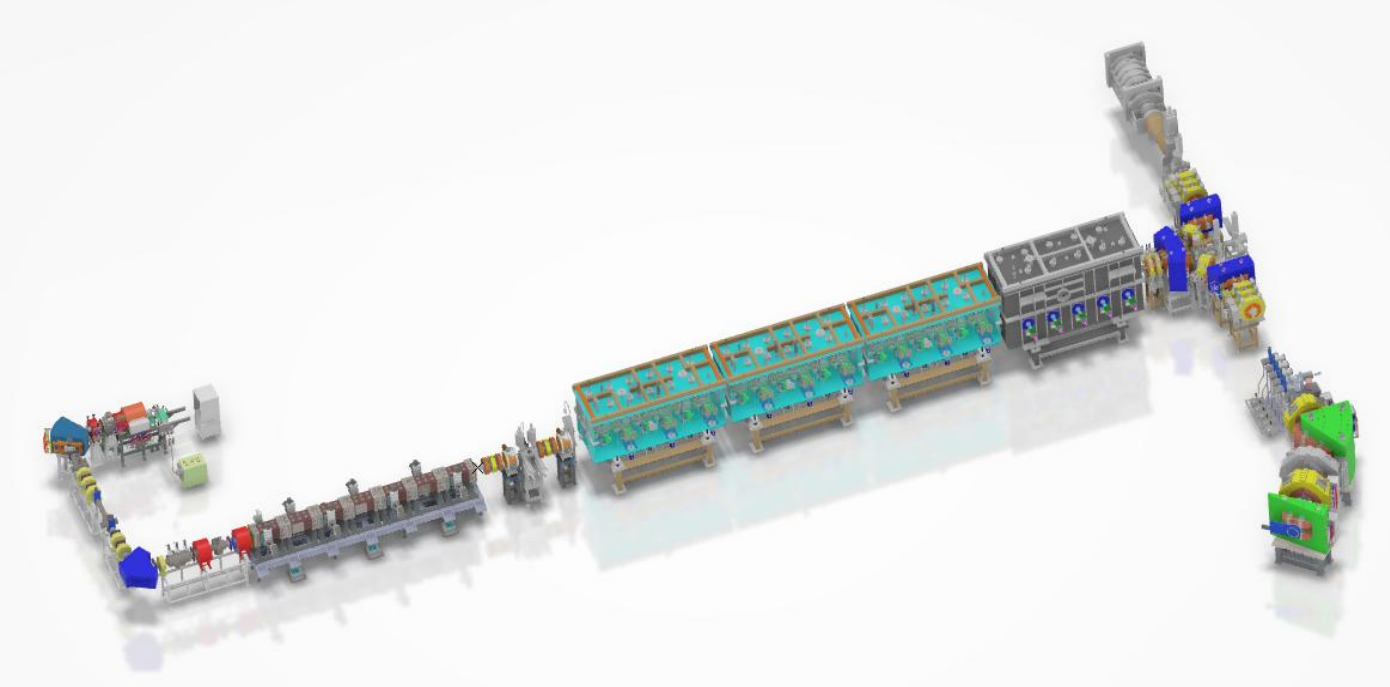

- consists of: ion source front-end system (FE), radio-frequency quadrupole accelerator (RFQ), medium energy beam transport (MEBT), superconducting cavity linac (SC), high energy beam transport (HEBT) and a gas-filled recoil separator-SHANS2

Experiment: About CAFE-II MEBT section

- CAFE2 MEBT section
  - located downstream of the RFQ exit
  - Three adjustable quadrupole
    - Focus - Defocus - Focus
  - Measurement device
    - Slit - Wire

Measurement device: Conventional devices are required to measure coupling information

- Algorithm inputs:
  - ① $g_j(u_j, u_j')$:
    - Measured 2D profile
    - More profiles enable higher reconstruction accuracy
  - ② Coordinate transformation matrix: A_j
    - $$\begin{bmatrix} u_j \\ u_j' \\ v_j \\ v_j' \end{bmatrix} = A_j \begin{bmatrix} x \\ x' \\ y \\ y' \end{bmatrix} = MM_j \begin{bmatrix} x \\ x' \\ y \\ y' \end{bmatrix}$$
    - $A\_j=MM\_j$
    - M_j: transmission matrix from the measurement points to the reconstruction points for the j-th profile
    - M: Mapping matrix from phase space to measurement coordinates

- Profiles containing coupling information must be measured in real space
- Identify appropriate measurement techniques
  - No additional coupling components are required
  - Conventional 2D measurement devices suffices

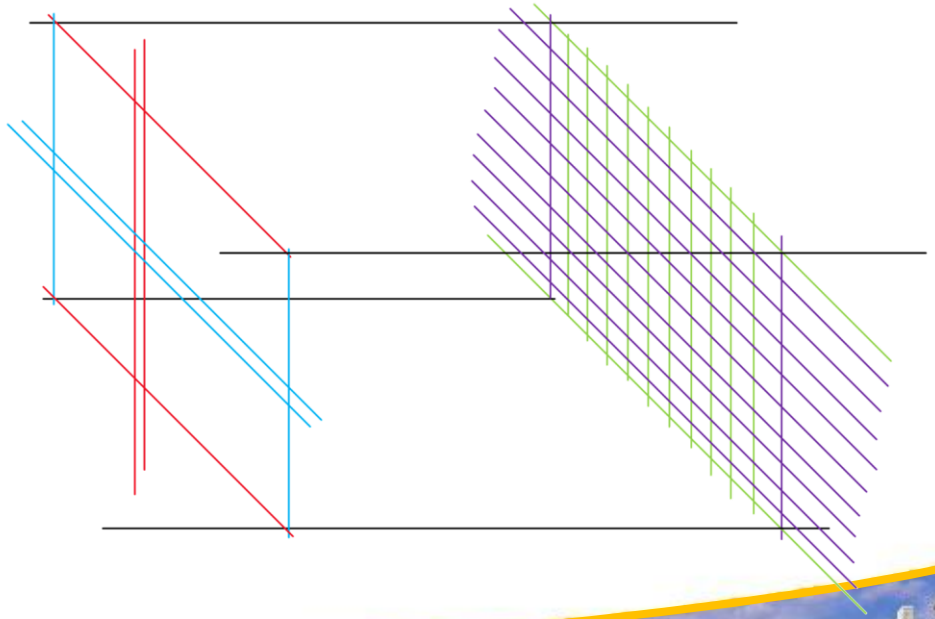

Measurement device: Parallel-scan and perpendicular-scan

2D Profiles Measured in Real Space as Reconstruction Constraints

- Acquisition of 2D profiles using parallel and perpendicular scans
- Parallel-scan
  - Using mutually parallel slit and wire
  - Measuring x or y-directional information
- perpendicular-scan
  - Using mutually perpendicular slit and wire
  - Measuring coupling information
- Front-slit data: suffix i; rear-slit data: suffix f
- Adjusting the magnet strength once scans four profiles:

$$(x_i, x_f), (y_i, y_f), (x_i, y_f), (y_i, x_f)$$

Measurement device: The coupling information is measurable

■ Linear mapping between phase space and real space

$$\begin{pmatrix} x_i \\ x_f \\ y_i \\ y_f \end{pmatrix} = \begin{pmatrix} 1 & 0 & 0 & 0 \\ 1 & L & 0 & 0 \\ 0 & 0 & 1 & 0 \\ 0 & 0 & 1 & L \end{pmatrix} \begin{pmatrix} x_i \\ x_i' \\ y_i \\ y_i' \end{pmatrix}$$

- 4D space(x_i, x_f, y_i, y_f):
  - All coordinate axes mutually orthogonal
  - All coordinates are real-space coordinates:
    - i: at the front slit position
    - f: at the back slit position
  - measured: $(x_i, x_f), (y_i, y_f), (x_i, y_f), (y_i, x_f)$
- (x_i, x_i', y_i, y_i'): 4D transverse phase space at the front slit position

■ Relationships of second-order statistical quantities

$$\begin{cases} \langle x_i y_f \rangle = (a_{33} + La_{34})(a_{11}\langle xy \rangle + a_{12}\langle x'y \rangle) \\ \quad +(a_{34} + La_{44})(a_{11}\langle xy' \rangle + a_{12}\langle x'y' \rangle) \\ \langle y_i x_f \rangle = (a_{11} + La_{22})(a_{33}\langle xy \rangle + a_{34}\langle xy' \rangle) \\ \quad +(a_{12} + La_{22})(a_{33}\langle x'y \rangle + a_{34}\langle x'y' \rangle) \end{cases}$$

- Two sets of magnet strengths can determine the covariance
- a_{ij}: elements of transport matrix

$$\begin{pmatrix} a_{11} & a_{12} & 0 & 0 \\ a_{21} & a_{22} & 0 & 0 \\ 0 & 0 & a_{33} & a_{34} \\ 0 & 0 & a_{43} & a_{44} \end{pmatrix} \begin{pmatrix} x_{re} \\ x_{re}' \\ y_{re} \\ y_{re}' \end{pmatrix} = \begin{pmatrix} x_i \\ x_i' \\ y_i \\ y_i' \end{pmatrix}$$

- $(x_{re}, x_{re}', y_{re}, y_{re}')$: 4D transverse phase space distribution at reconstruction point

Experiment: Reconstruct 4D transverse phase space in CAFE-II MEBT section

Beam parameters:

- Particle: Proton
- Energy: 1.33 MeV
- Current: 100/200/300 μA

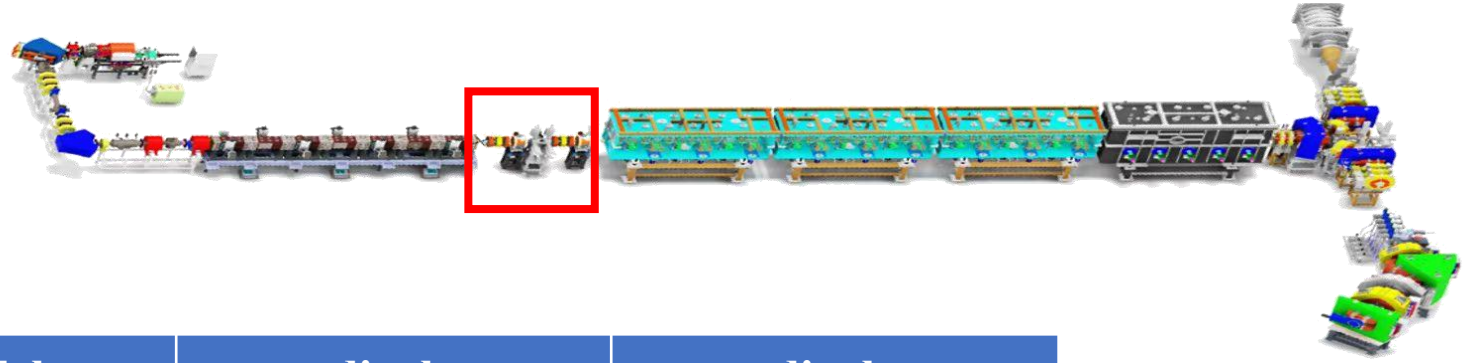

4 magnet settings per current step	Parallel scan: (slit x, wire x)	Parallel scan: (slit y, wire y)	perpendicular-scan: (slit x, wire y)	perpendicular-scan: (slit y, wire x)
66, -88, 68	✓[1]	✓[2]	✓[3]	✓[4]
56.4, 72.2, 59.3	×	×	✓[5]	✓[6]
55, 63, 42	×	×	✓[7]	✓[8]
38, 63, 55	×	×	✓[9]	✓[10]

- ✓: Profiles used in reconstruction
- ×: Unused profiles
- Measurement axis ID: [X]

Nonlinear Mapping Must Be Considered in this Experiment

- If only linear mapping is considered:
  - Reconstruction converges using profiles [1][2][3][4]
  - Reconstruction fails to converge using profiles [1][2][3][4][5][6]
- Nonlinear mapping originates from leakage fields of quadrupole

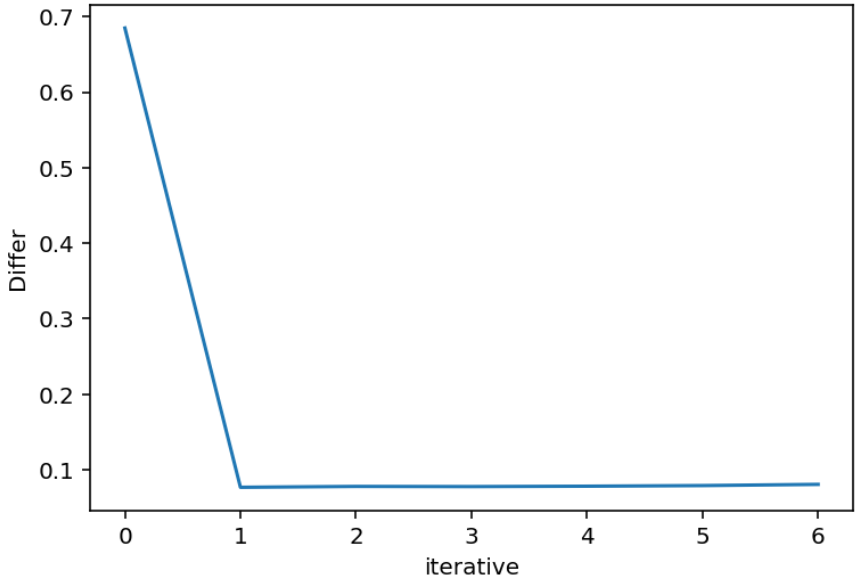

Convergence achieved when all profiles use the same magnet parameter set

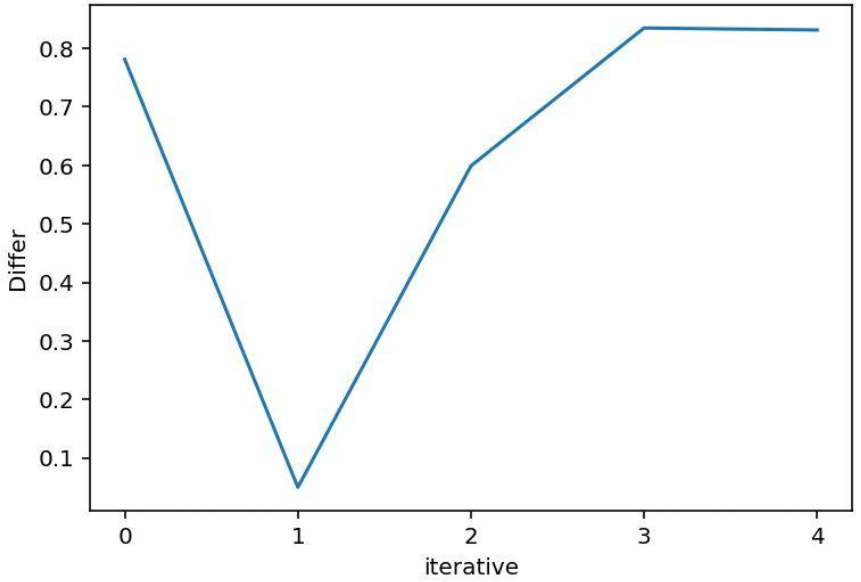

Instability occurs when profiles are generated from different magnet parameter iterations

Calculation of nonlinear mapping induced by fringe field: The expansion of nonlinear mapping

➢ Concerning arbitrary nonlinear mappings

$$(x, x', y, y') = f(x_0, x'_0, y_0, y'_0)$$

$$\begin{bmatrix} x \\ x' \\ y \\ y' \end{bmatrix} = \begin{bmatrix} a_{11} & a_{12} & a_{13} & a_{14} \\ a_{21} & a_{22} & a_{23} & a_{24} \\ a_{31} & a_{32} & a_{33} & a_{34} \\ a_{41} & a_{42} & a_{43} & a_{44} \end{bmatrix} \begin{bmatrix} x_0 \\ x'_0 \\ y_0 \\ y'_0 \end{bmatrix}$$

$$+ \begin{bmatrix} b_{11} & b_{12} & b_{13} & b_{14} & b_{15} & b_{16} & b_{17} & b_{18} & b_{19} & b_{110} \\ b_{21} & b_{22} & b_{23} & b_{24} & b_{25} & b_{26} & b_{27} & b_{28} & b_{29} & b_{210} \\ b_{31} & b_{32} & b_{33} & b_{34} & b_{35} & b_{36} & b_{37} & b_{38} & b_{39} & b_{310} \\ b_{41} & b_{42} & b_{43} & b_{44} & b_{45} & b_{46} & b_{47} & b_{48} & b_{49} & b_{410} \end{bmatrix} \begin{bmatrix} {x_0}^2 \\ x_0 x'_0 \\ x_0 y_0 \\ x_0 y'_0 \\ {x'_0}^2 \\ x'_0 y_0 \\ x'_0 y'_0 \\ {y_0}^2 \\ y_0 y'_0 \\ {y'_0}^2 \end{bmatrix}$$

$$+ M_{4*20} \cdot Cubic_{20} + M_{4*35} \cdot Quartic_{35} + \cdots M_{4*\frac{(4+r-1)!}{r!3!}} \cdot r_{\frac{(4+r-1)!}{r!3!}} + \cdots$$

➢ The quantity of characteristic terms at the r-th order

$$C_{n+r-1}^{r} = \frac{(n+r-1)!}{r!\,(n-1)!}$$

- n: the dimensionality parameter, which equals 4 in the context of four-dimensional transverse phase space
- r: The order of expansion

➢ The coefficient matrix of the r-th order:

$$M_{(4,\frac{(4+r-1)!}{r!3!})}$$

➢ The solution methodology:

- The number of particles tracked satisfies the inequality: **Quantity tracked** $\geq \sum_{i=1}^{r} \frac{(3+r)!}{r!3!}$
- Compute all $\sum_{i=1}^{r}(4 \cdot \frac{(3+r)!}{r!3!})$ coefficients

Calculation of nonlinear mapping induced by field leakage: Tracking lattice distribution

- Simulation using field models in simulation software
- Solving equation systems based on particle entry and exit coordinates

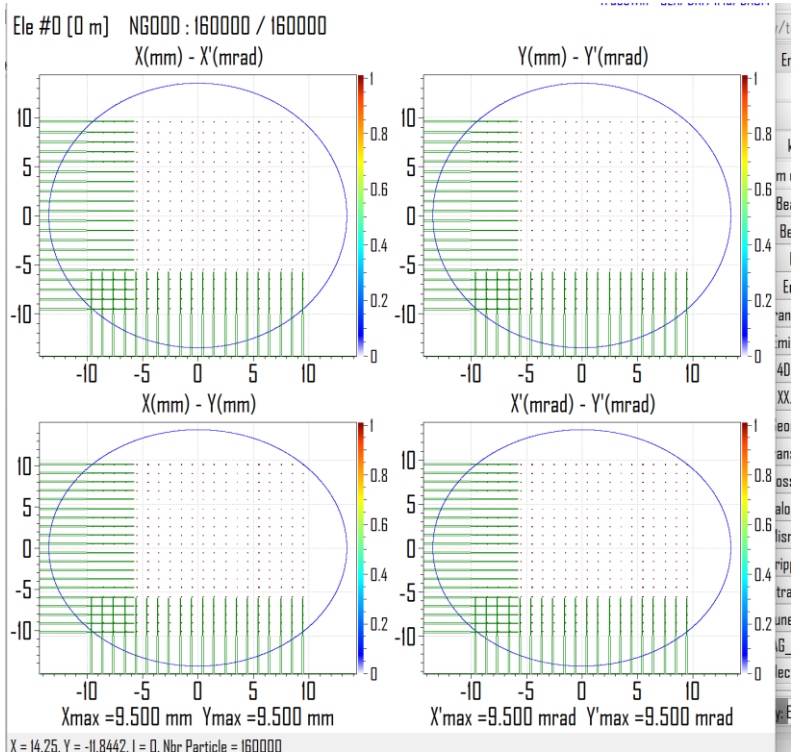

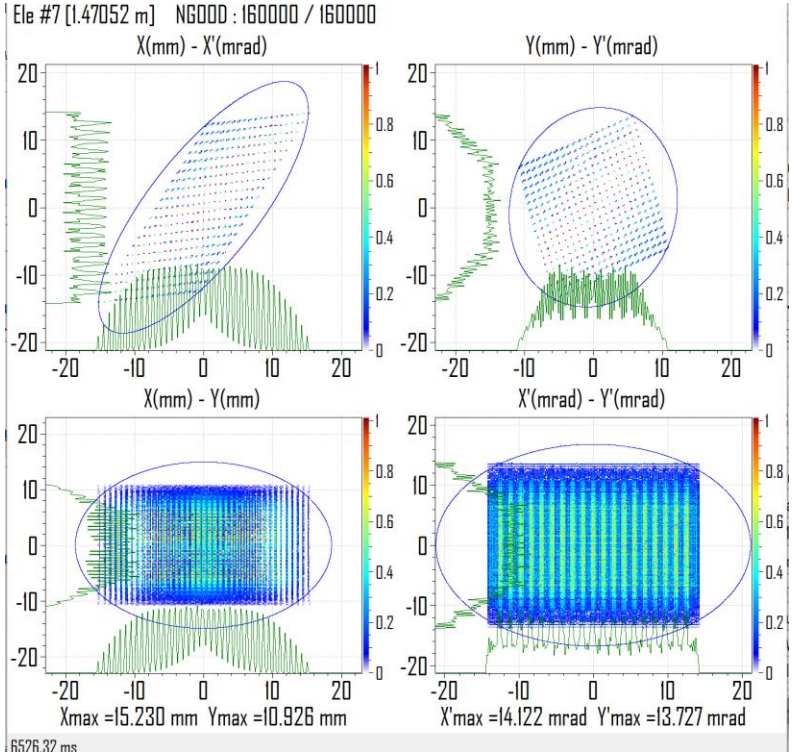

Alternative approaches: Derive nonlinear map from the field map

- a simple particle coordinate tracking method was used to derive the mapping function
- Subsequently, the mapping function will be recalculated using a field model instead

➢ Numerous readily available algorithms can derive nonlinear mapping functions from field models

Code Name	Algorithm / Basis	Primary Application
COSY INFINITY	Differential Algebra (DA)	High-order beam dynamics & complex nonlinear optics
IMPACT (T/Z)	3D PIC Code	Accelerating cavities, magnetic elements + space charge
PTC	Polymorphic Tracking	Precise tracking within MAD-X, fringe fields
Bmad	Object-oriented Library	Custom 3D mesh handling for particle maps
RF-Track	Time-domain Tracking	Beam transport optimization in linacs & cavities

Experiment: Result presentation(300uA)

- Constraints No.[1] to No.[10]

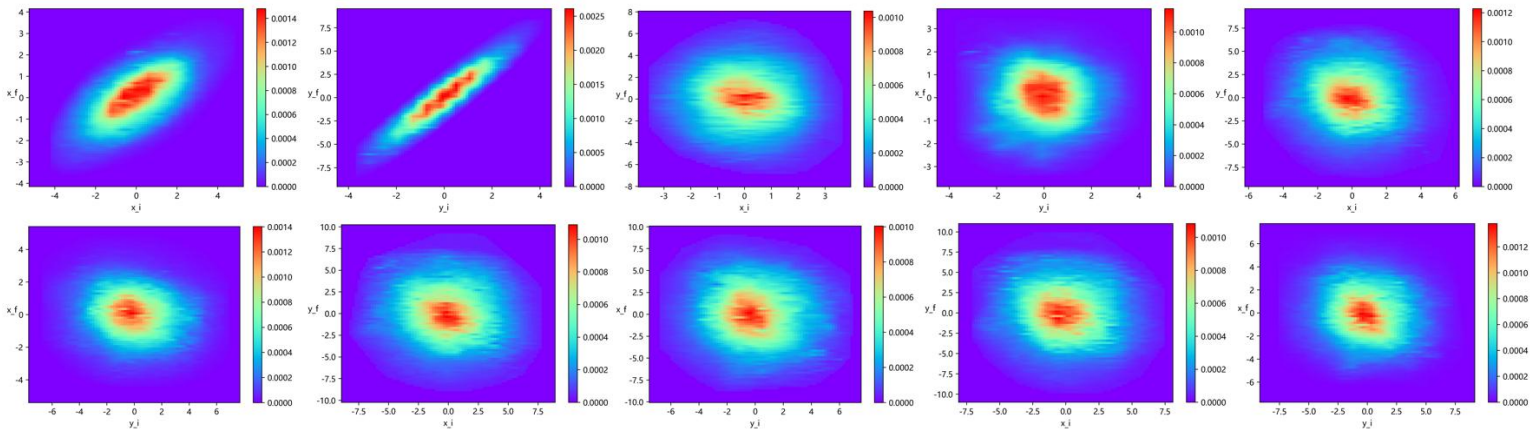

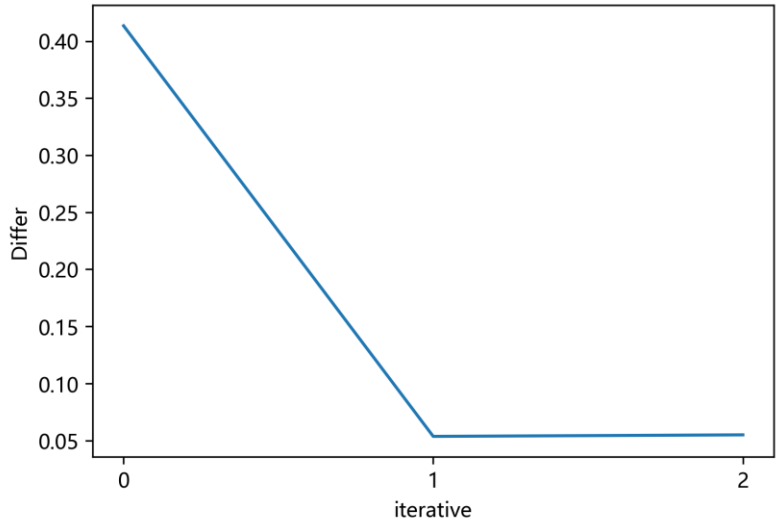

- Projection of the reconstructed result onto directions [1] to [10]

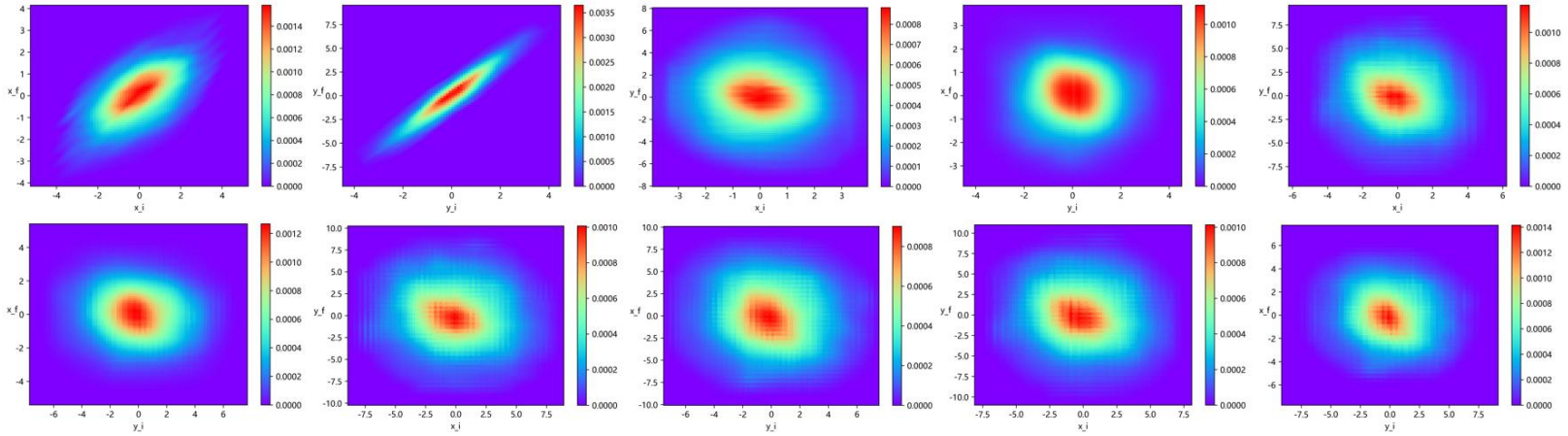

$$\frac{1}{20}\left(\sum_{j=1}^{10}\int\left|Constraints_j - \text{Projection}_j\right|\right) = 0.053659270534929 57$$

Experiment: Result presentation(200uA)

- Constraints No.[1] to No.[10]

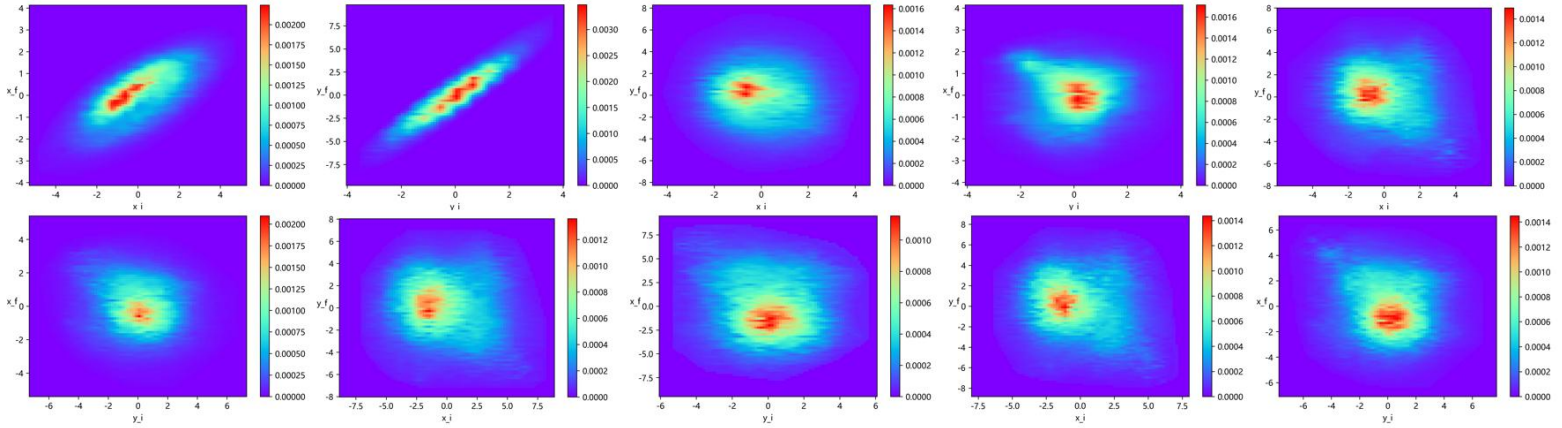

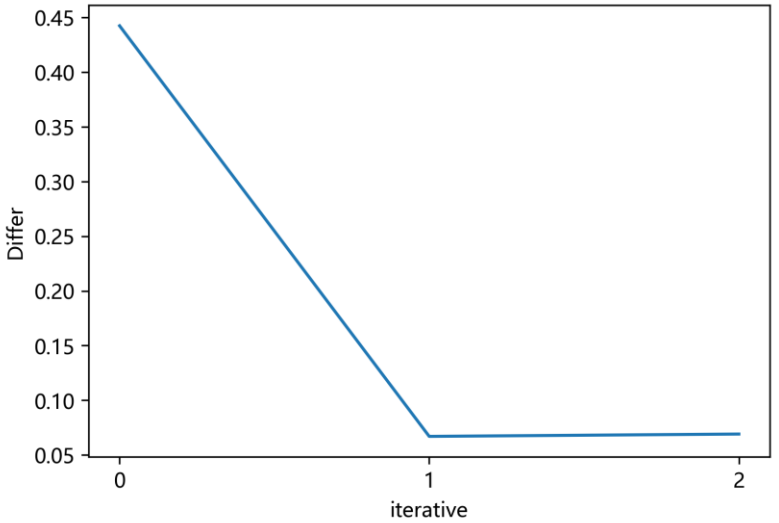

- Projection of the reconstructed result onto directions [1] to [10]

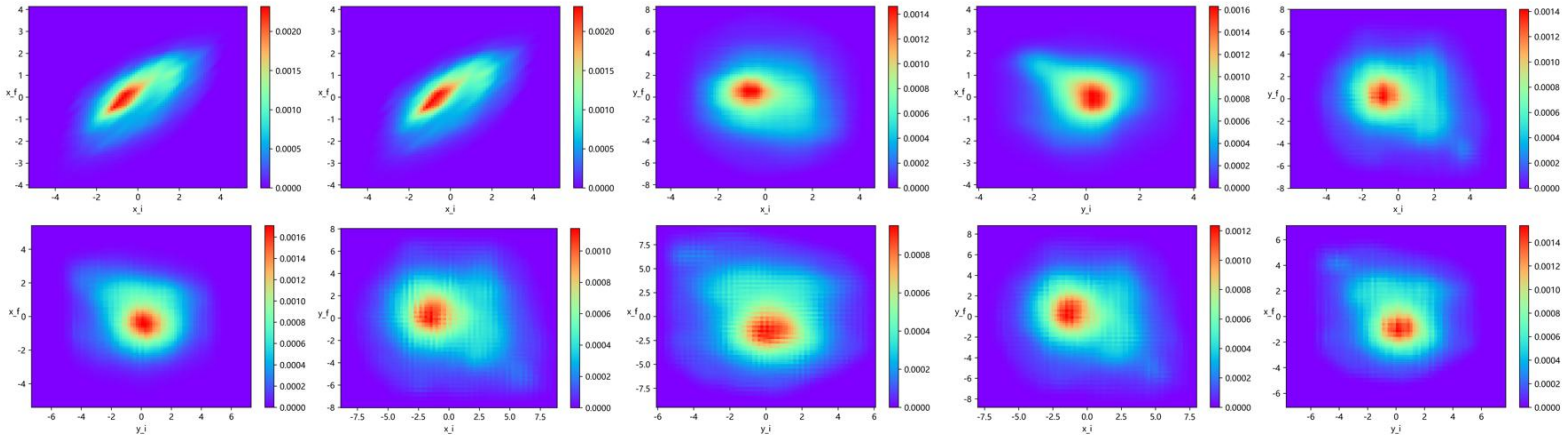

$$\frac{1}{20}\left(\sum_{j=1}^{10}\int\left|Constraints_j - \text{Projection}_j\right|\right) = 0.06702086964054674$$

Experiment: Result presentation(100uA)

- Constraints No.[1] to No.[10]

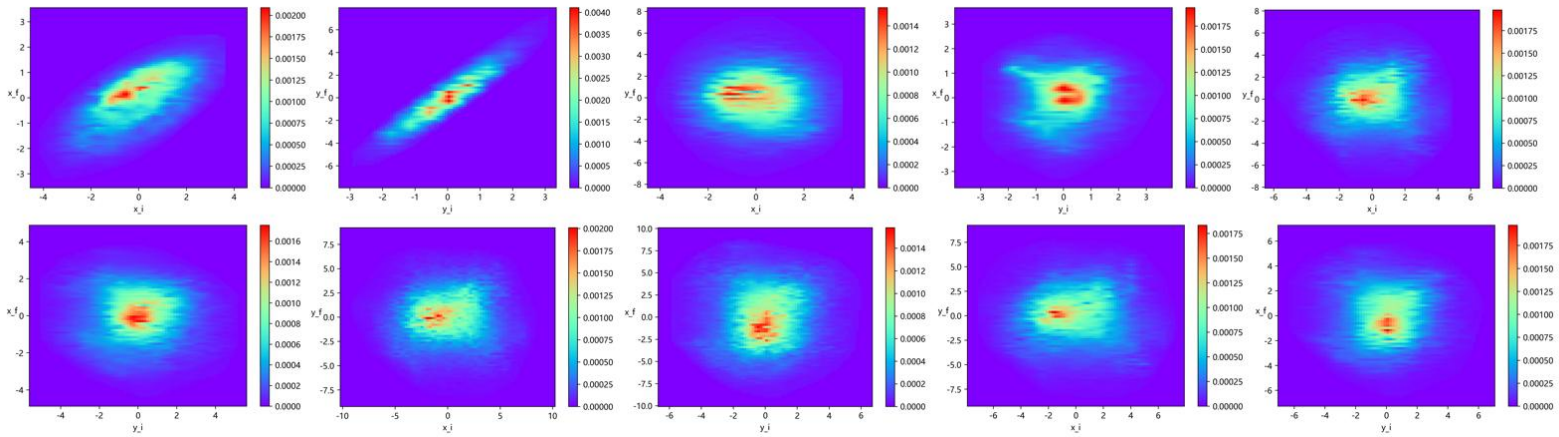

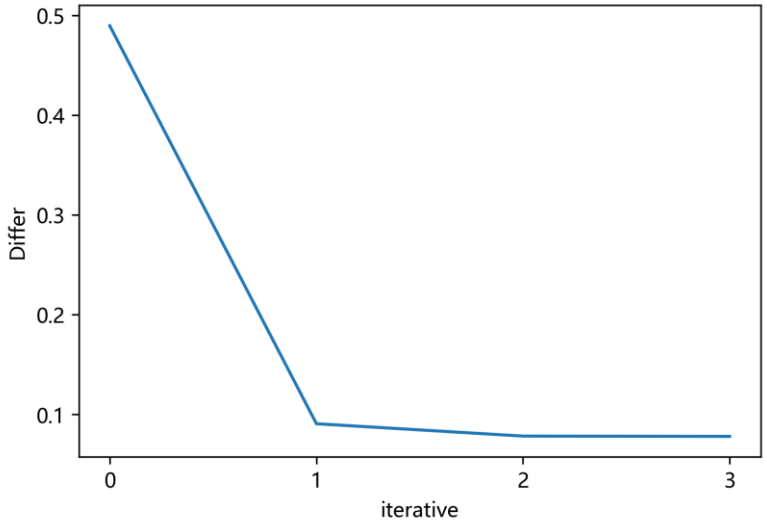

- Projection of the reconstructed result onto directions [1] to [10]

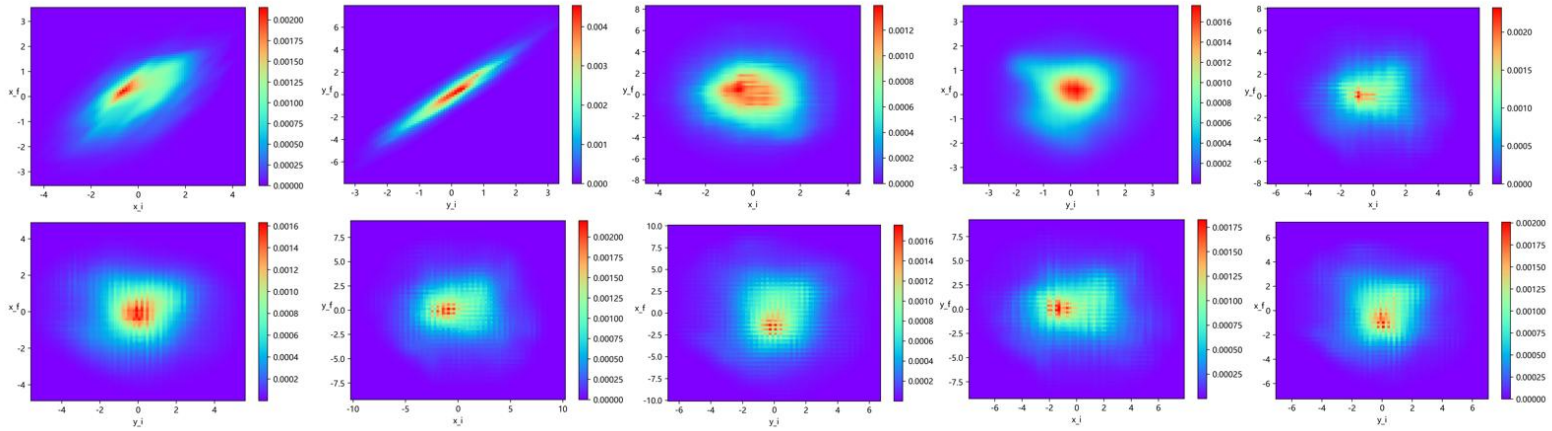

$$\frac{1}{20}\left(\sum_{j=1}^{10}\int\left|Constraints_j - \text{Projection}_j\right|\right) = 0.07774037280402595$$

Thanks!